

## Article

# Interconversion and Removal of Inorganic Nitrogen Compounds via UV Irradiation

Alejandro M. Senn<sup>1,\*</sup> and Natalia Quici<sup>1,2,\*</sup> 

<sup>1</sup> División Química de la Remediación Ambiental, Centro Atómico Constituyentes, CNEA, CONICET, Gral. Paz 1499, San Martín, Buenos Aires 1650, Argentina

<sup>2</sup> Centro de Tecnologías Químicas, Departamento de Ingeniería Química, FRBA-UTN, Buenos Aires 1041, Argentina

\* Correspondence: amsenn@cnea.gov.ar (A.M.S.); nquici@cnea.gov.ar (N.Q.)

**Abstract:** Dissolved inorganic nitrogen (DIN) species are key components of the nitrogen cycle and are the main nitrogen pollutants in groundwater. This study investigated the interconversion and removal of the principal DIN compounds ( $\text{NO}_3^-$ ,  $\text{NO}_2^-$  and  $\text{NH}_4^+$ ) via UV light irradiation using a medium-pressure mercury lamp. The experiments were carried out systematically at relatively low nitrogen concentrations (1.5 mM) at varying pHs in the presence and absence of oxygen to compare the reaction rates and suggest the reaction mechanisms.  $\text{NO}_3^-$  was fully converted into  $\text{NO}_2^-$  at a pH > 3 in both oxic and anoxic conditions, and the reaction was faster when the pH was increased following a first-order kinetic at pH 11 ( $k = 0.12 \text{ min}^{-1}$ ,  $R^2 = 0.9995$ ).  $\text{NO}_2^-$  was partially converted into  $\text{NO}_3^-$  only at pH 3 and in the presence of oxygen and was stable at an alkaline pH. This interconversion of  $\text{NO}_3^-$  and  $\text{NO}_2^-$  did not yield nitrogen loss in the solution. The addition of formic acid as an electron donor led to the reduction of  $\text{NO}_3^-$  to  $\text{NH}_4^+$ . Conversely,  $\text{NH}_4^+$  was converted into  $\text{NO}_2^-$ ,  $\text{NO}_3^-$  and to an unidentified subproduct in the presence of  $\text{O}_2$  at pH 10. Finally, it was demonstrated that  $\text{NO}_2^-$  and  $\text{NH}_4^+$  react via UV irradiation with stoichiometry 1:1 at pH 10 with the total loss of nitrogen in the solution. With these results, a strategy to remove DIN compounds via UV irradiation was proposed with the eventual use of solar light.

**Keywords:** nitrogen removal; inorganic nitrogen; photolysis; reactive nitrogen species



**Citation:** Senn, A.M.; Quici, N.

Interconversion and Removal of Inorganic Nitrogen Compounds via UV Irradiation. *ChemEngineering* **2023**, *7*, 79. <https://doi.org/10.3390/chemengineering7050079>

Academic Editors: Thomas Grützner, Bernhard Seyfang and Ori Lahav

Received: 7 July 2023

Revised: 28 July 2023

Accepted: 28 August 2023

Published: 31 August 2023



**Copyright:** © 2023 by the authors. Licensee MDPI, Basel, Switzerland. This article is an open access article distributed under the terms and conditions of the Creative Commons Attribution (CC BY) license (<https://creativecommons.org/licenses/by/4.0/>).

## 1. Introduction

The chemical element nitrogen (N) is a key component of life. Its most abundant form on Earth is atmospheric dinitrogen ( $\text{N}_2$ ). However,  $\text{N}_2$  is unavailable for most organisms, making N a limiting nutrient. Therefore, N compounds in nature can be classified into two groups: nonreactive N ( $\text{N}_2$ ) and reactive N ( $\text{N}_r$ ).  $\text{N}_r$  includes all biologically, photochemically, and radiatively active N compounds in the Earth's atmosphere and biosphere [1].  $\text{N}_r$  can be found in both organic and inorganic compounds. Organic compounds include urea, amines, proteins, and nucleic acids. Inorganic compounds can be gaseous (e.g., nitrous oxide ( $\text{N}_2\text{O}$ ), nitrogen oxide (NO) and nitrogen dioxide ( $\text{NO}_2$ ), with the last two known as  $\text{NO}_x$ ) and also can be present in soil and water. The most common dissolved inorganic nitrogen (DIN) compounds in water are nitrate ( $\text{NO}_3^-$ ), nitrite ( $\text{NO}_2^-$ ) and ammonium ( $\text{NH}_4^+$ ). In particular,  $\text{NO}_3^-$  is the main nitrogen groundwater pollutant [2].

In the natural cycle of N,  $\text{N}_2$  is converted into  $\text{N}_r$  by lightning and by biological nitrogen fixation. The reverse reaction in the cycle converts organic N and  $\text{NH}_4^+$  into  $\text{NO}_2^-$  and  $\text{NO}_3^-$  (nitrification) and then to  $\text{N}_2$  (denitrification). A few decades ago, these opposite processes were approximately equal. However, in recent times, anthropogenic activity [3] has led to an imbalance between these processes, resulting in the accumulation of  $\text{N}_r$  in the environment. This includes the industrial Haber–Bosch process that converts  $\text{N}_2$  into  $\text{NH}_3$  used in the synthesis of fertilizers for food production and the fossil-fuel

combustion that converts fossil N into  $\text{NO}_x$  [4]. To overcome the  $\text{N}_r$  accumulation, the natural nitrification/denitrification process has been implemented in wastewater treatment plants [5]. Recently, another biological process, autotrophic anaerobic ammonium oxidation (Anammox), has been used on a large scale [6]. In this process,  $\text{NH}_4^+$  is oxidized with  $\text{NO}_2^-$  to yield  $\text{N}_2$  via a biologically mediated process. DINs can also be removed using traditional physicochemical treatments, such as ion exchange, adsorption, etc. [7].

Therefore, DINs are key compounds in the nitrogen cycle and water treatment technologies. In particular, the photocatalytic reduction of  $\text{NO}_3^-$  into  $\text{N}_2$  is emerging as an alternative to the removal of nitrogen from water [7].  $\text{TiO}_2$  is the most studied photocatalyst for this purpose but the interconversion of inorganic nitrogen compounds can also be achieved without it via simple UV irradiation [8]. The absorption spectra of  $\text{NO}_3^-$  and  $\text{NO}_2^-$  are dominated by intense  $\pi \rightarrow \pi^*$  bands at 200 nm ( $\epsilon = 9900 \text{ M}^{-1} \text{ cm}^{-1}$ ) and 205 nm ( $\epsilon = 5500 \text{ M}^{-1} \text{ cm}^{-1}$ ), respectively. But they also present weaker  $n \rightarrow \pi^*$  bands at 310 nm ( $\epsilon = 7.4 \text{ M}^{-1} \text{ cm}^{-1}$ ) and 360 nm ( $\epsilon = 22.5 \text{ M}^{-1} \text{ cm}^{-1}$ ), respectively. These last bands can absorb solar radiation ( $\lambda > 295 \text{ nm}$ ), and they are important not only for solar-based technologies but also for processes initiated by sunlight in natural waters and in atmospheric aerosols [9]. Brown carbon aerosols are light-absorbing particles primarily originating from biomass combustion. Comprising near-UV-absorbing organic compounds mixed with  $\text{NO}_3^-$  within atmospheric aerosols, these aerosols are thought to contribute to the presence of nitrous acid in the atmosphere through the photolysis of  $\text{NO}_3^-$  into  $\text{NO}_2$  and  $\text{NO}_2^-$  [10].

Although  $\text{NH}_4^+$  does not absorb significantly within the UV-vis spectra, it can be oxidized through photocatalytic methods [11]. The removal of  $\text{NH}_4^+/\text{NH}_3$  via oxidation poses a significant challenge due to its high stability and water solubility. Photocatalytic oxidation using  $\text{TiO}_2$  (P25), particularly at high pH conditions, has been successful at converting  $\text{NH}_4^+/\text{NH}_3$  into  $\text{N}_2$  [12]. In this investigation, we explored  $\text{NH}_4^+/\text{NH}_3$  oxidation via irradiation in the presence of oxygen, omitting the use of a catalyst.

Usually, irradiation experiments have been undertaken to study DIN species separately. This work attempts to describe systematically the main features arising from the irradiation of DIN species by applying similar conditions but also through the simultaneous irradiation of  $\text{NO}_2^-$  and  $\text{NH}_4^+$ . In this specific scenario, prior research [13] demonstrates that photolysis exhibits superior performance compared to the photocatalytic process for nitrogen removal. The focus was placed on the main DIN compounds ( $\text{NO}_3^-$ ,  $\text{NO}_2^-$  and  $\text{NH}_4^+$ ) in a relatively low total nitrogen concentration (1.5 mM).

The irradiation of DINs produces nitrogen radicals and  $\text{OH}^\bullet$ , which subsequently facilitates the oxidation of organic matter. This approach has garnered attention for its potential in addressing environmental challenges, particularly in the oxidation of emerging contaminants of concern (CECs) through UV irradiation when residual  $\text{NO}_2^-$  is present [14]. In this study, formic acid ( $\text{HCOOH}$ ) was selected as the target organic compound for oxidation due to its convenient mineralization and traceable degradation process.

The irradiation was aimed to excite the  $n \rightarrow \pi^*$  absorption bands of the compounds, which have implications in solar applications. For this purpose, a medium-pressure mercury lamp (main emission bands between 313 and 436 nm) was used in contrast with other studies that employ low-pressure mercury lamps (maximum emission at 254 nm) that excite the  $\pi \rightarrow \pi^*$  bands principally [15]. A discussion was completed about the interconversion of DINs, the possible intermediates and the potential conversion into  $\text{N}_2$  for the nitrogen removal from water.

## 2. Materials and Methods

### 2.1. Chemicals

Solutions were prepared with  $\text{KNO}_3$  (>99%, Mallinkrodt),  $\text{NaNO}_2$  (>99%, Merck),  $\text{NH}_4\text{OH}$  (30%, Anedra) and  $\text{HCOOH}$  (88%, Biopack) and used without further purification. For pH adjustments,  $\text{H}_2\text{SO}_4$  (Biopack) or  $\text{NaOH}$  (Biopack) was used. Analytical calibration standards of  $\text{KNO}_3$ ,  $\text{NaNO}_2$  and  $\text{NH}_4\text{Cl}$  were obtained from ChemLab. All experiments

were performed with MilliQ water (resistivity = 18 M $\Omega$  cm), and all mentioned chemicals were analytical grade or superior.

## 2.2. Irradiation Experiments

Irradiation experiments were performed in an immersion well reactor (Figure 1) consisting of a thermostatted (298 K) annular reactor (130 mm length, 57 mm external diameter, 48 mm internal diameter, 160 mL total cell volume). The irradiation source was a medium-pressure mercury lamp installed inside the reactor (Photochemical Reactors Ltd., Reading, UK). This lamp emits radiation between 300 and 440 nm with main peaks at 313, 366, 404 and 436 nm (Figure S1 in Supplementary Material includes the emission spectrum of the medium-pressure Hg lamp together with the absorption bands of NO<sub>3</sub><sup>-</sup> and NO<sub>2</sub><sup>-</sup>). Actinometric measurements were performed using the ferrioxalate method. An incident photon flux per unit volume ( $q_p/V$ , where  $q_p$  is the incident photon flux, and  $V$  is the irradiated volume) of  $3.2 \times 10^{-4}$   $\mu\text{einstein s}^{-1} \text{L}^{-1}$  was calculated. In all cases, 200 mL of NO<sub>3</sub><sup>-</sup> (1.5 mM), NO<sub>2</sub><sup>-</sup> (1.5 mM), NH<sub>3</sub>/NH<sub>4</sub><sup>+</sup> (1.5 mM), NO<sub>2</sub><sup>-</sup> (0.75 mM) + NH<sub>3</sub>/NH<sub>4</sub><sup>+</sup> (0.75 mM) or NO<sub>3</sub><sup>-</sup> (1.2 mM) + HCOOH (30 mM) solutions was adjusted to the desired pH using dropwise addition of H<sub>2</sub>SO<sub>4</sub> (0.5 M) or NaOH (0.5 M) into the reservoir where argon or oxygen (0.2 L min<sup>-1</sup>) was constantly bubbled. All the experiments were performed at  $25.0 \pm 0.1$  °C. Solutions in the reservoir were magnetically stirred throughout the reaction time. Samples (1 mL) were periodically extracted for analysis, and the pH was measured. All runs were performed at least in duplicate, and the results were averaged. The experimental error was never higher than 10%.

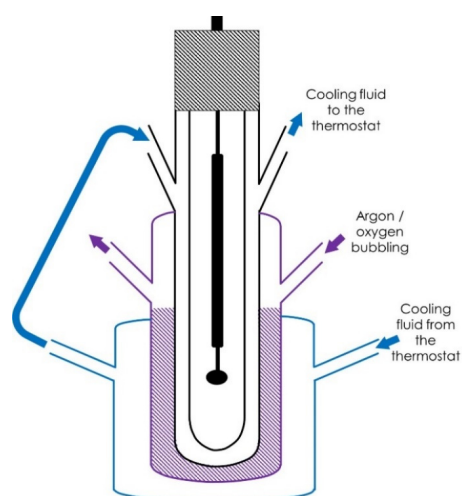


**Figure 1.** Scheme of the irradiation setup.

## 2.3. Analytical Techniques

Periodically withdrawn samples were conditioned to determine [NO<sub>3</sub><sup>-</sup>], [NO<sub>2</sub><sup>-</sup>], [NH<sub>4</sub><sup>+</sup>] and [HCOOH]. The concentrations of NO<sub>3</sub><sup>-</sup>, NO<sub>2</sub><sup>-</sup> and NH<sub>4</sub><sup>+</sup> were measured spectrophotometrically using the standard methods SM-4500-NO<sub>3</sub>-E [16], SM-4500-NO<sub>2</sub>-B [17] and SM-4500-NH<sub>3</sub>-F [18], respectively, employing an HP8453A spectrophotometer (Hewlett-Packard) with UV detection. HCOOH concentration was determined using a Shimadzu 5000 A TOC analyzer in the non-purgeable organic carbon (NPOC) mode.

## 3. Results and Discussion

### 3.1. Irradiation of NO<sub>3</sub><sup>-</sup>

Figure 2 shows the removal of aqueous NO<sub>3</sub><sup>-</sup> (dashed lines) and the parallel NO<sub>2</sub><sup>-</sup> formation (solid lines) due to the irradiation of the nitrate solutions in a pH range from 3 to 11 with a medium-pressure mercury lamp in anoxic conditions. The reaction rate

increased when varying from an acid to alkaline solution, yielding  $\text{NO}_2^-$  as the main product (Equation (1)).

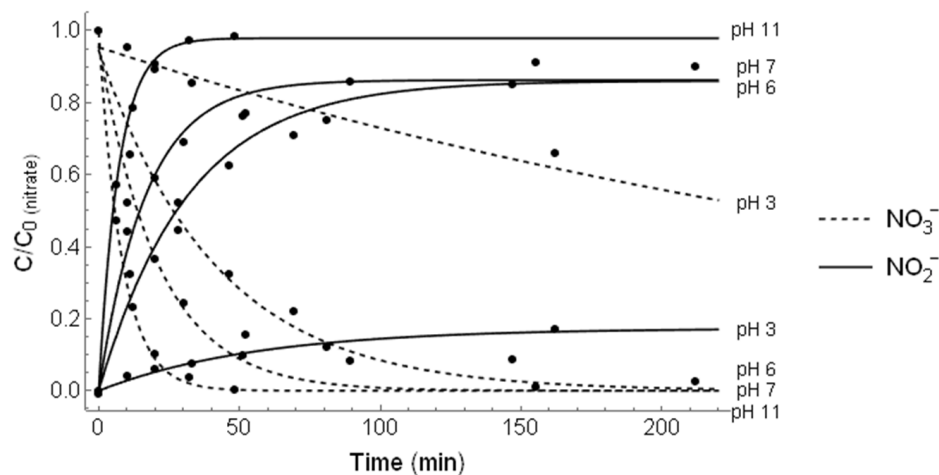


**Figure 2.**  $\text{NO}_3^-$  (dashed lines) and  $\text{NO}_2^-$  profiles (solid lines) vs. time obtained after the irradiation of  $\text{NO}_3^-$  (1.5 mM) at varying pH conditions. The solutions were continuously purged with argon.

At a neutral and acidic pH, the nitrogen mass balance of  $\text{NO}_3^-$ ,  $\text{NO}_2^-$  and  $\text{NH}_4^+$  in the solution during irradiation indicates that they did not account for 100% of the nitrogen introduced in the system as  $\text{NO}_3^-$ . This discrepancy is likely attributed to a loss of nitrogen from the aqueous phase. As presented in Table 1, the nitrogen recovery considers the total nitrogen found in the solution after the reaction (i.e., nitrogen originating from  $\text{NO}_3^-$ ,  $\text{NO}_2^-$  and  $\text{NH}_4^+$ ). The observed behavior concerning the influence of the solution pH is consistent with findings reported by other authors who have utilized a low-pressure mercury lamp [15].

**Table 1.** Kinetics of the photo reduction of  $\text{NO}_3^-$  at varying pH conditions. The data presented were calculated by performing a mathematical adjustment of the kinetic curves presented in Figure 2. Nitrogen recovery was calculated as  $100 \times ([\text{NO}_3^-]_f + [\text{NO}_2^-]_f + [\text{NH}_3]_f) / [\text{NO}_3^-]_i$ .

Purge	pH	Kinetic Rate Constant ( $\text{min}^{-1}$ )	Correlation Coefficient ( $R^2$ )	Nitrogen Recovery (%)
Argon	3	0.003	0.9980	83
	6	0.024	0.9917	93
	7	0.048	0.9879	92
	11	0.121	0.9995	99
Oxygen	10	0.084	0.9919	92

The total reduction of  $\text{NO}_3^-$  to  $\text{NO}_2^-$  was also confirmed in oxic conditions at an alkaline pH (Table 1), indicating that the presence of oxygen in the system did not affect the reduction of  $\text{NO}_3^-$ .

The observed pH dependence could be explained by the formation of peroxyntrous acid ( $\text{ONOOH}$ )/peroxynitrite ( $\text{ONOO}^-$ ) species considered to be one of the main intermediates of the photo reduction of  $\text{NO}_3^-$  [7].  $\text{ONOOH}$  is unstable, and it isomerizes to  $\text{NO}_3^-$  (Equation (2)), thereby reversing the reaction (1) [19]. This acid has a  $\text{pK}_a = 6.5$ ; therefore, at pH higher than 6.5,  $\text{ONOO}^-$  predominates, and the reaction continues to yield  $\text{NO}_2^-$  without reversing to  $\text{NO}_3^-$ .



### 3.2. Irradiation of $\text{NO}_2^-$

The oxidation of  $\text{NO}_2^-$  into  $\text{NO}_3^-$  through irradiation was partially achieved at pH 3 in the presence of  $\text{O}_2$ . In these conditions, 30% of  $\text{NO}_2^-$  (1.5 mM) was converted into  $\text{NO}_3^-$  within 2 h (Figure 3). Initially, when the  $\text{NO}_2^-$  solutions were prepared at pH 3, a rapid dark reaction leading to the oxidation of  $\text{NO}_2^-$  into  $\text{NO}_3^-$  was observed. Therefore, experiments at this pH were initiated with the presence of  $\text{NO}_3^-$ , as shown in Figure 3. In contrast, at a higher pH or in the absence of  $\text{O}_2$ , this reaction was not significant, indicating the stability of  $\text{NO}_2^-$  in the dark.

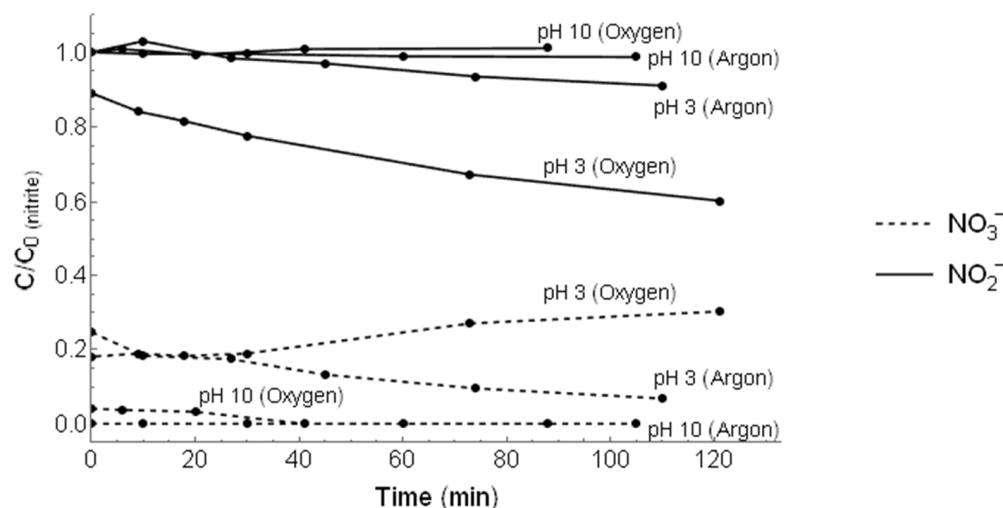


**Figure 3.**  $\text{NO}_3^-$  (dashed lines) and  $\text{NO}_2^-$  (solid lines) profiles vs. time obtained after the irradiation of  $\text{NO}_2^-$  (1.5 mM). The reaction was performed at pH 3 and pH 10 with and without  $\text{O}_2$ .

In an aqueous solution, nitrous acid ( $\text{HNO}_2$ ) exists in equilibrium with  $\text{NO}_2^-$  with a  $\text{pK}_a = 3.4$  (Equation (3)).



When exposed to 355 nm irradiation, both species undergo a similar photolytic process, with the acid form exhibiting a higher quantum yield ( $\phi_{355 \text{ nm}}^{\text{HNO}_2} = 0.4$  vs.  $\phi_{355 \text{ nm}}^{\text{NO}_2^-} = 0.025$  respectively) [7,20]. This disparity in quantum yields could explain the observed oxidation only in acidic conditions (Equations (4) and (5)).



### 3.3. Irradiation of $\text{NH}_3/\text{NH}_4^+$

The removal of aqueous  $\text{NH}_3/\text{NH}_4^+$  via irradiation was observed at a high pH (Figure 4) in the presence of oxygen in contrast to the  $\text{NO}_2^-$  oxidation that only took place at a low pH (Figure 3). At pH 10, 72% of  $\text{NH}_3/\text{NH}_4^+$  (1.5 mM) was converted mainly into an unidentified compound. The concentrations of  $\text{NO}_3^-$  and  $\text{NO}_2^-$  were low and constant throughout the experiment, suggesting that these compounds were reaction intermediates in a steady-state mechanism. The reaction was not observed at a pH lower than 7 (kinetic curves not shown) or in the absence of  $\text{O}_2$ .

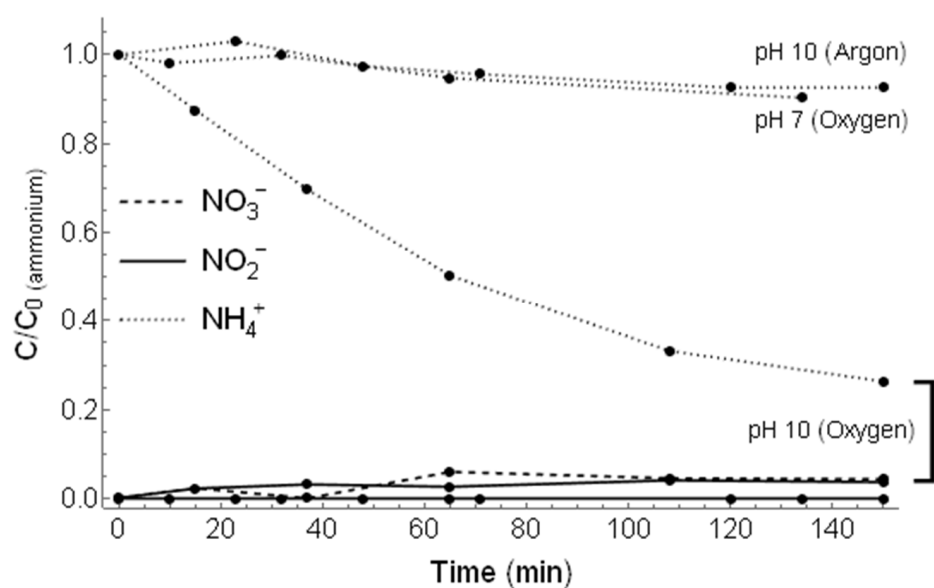
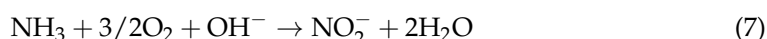


**Figure 4.**  $\text{NH}_4^+$  (dotted lines),  $\text{NO}_3^-$  (dashed lines) and  $\text{NO}_2^-$  (solid lines) profiles vs. time for the irradiation of  $\text{NH}_3/\text{NH}_4^+$  (1.5 mM) in oxic and anoxic conditions. The solutions were purged with oxygen and argon, respectively.

Unlike  $\text{NO}_3^-$  and  $\text{NO}_2^-$ ,  $\text{NH}_3/\text{NH}_4^+$  do not absorb light in the emission range of the medium-pressure mercury lamp. Therefore, the direct photolysis of these species was ruled out. Nevertheless, hydroxyl radical ( $\text{HO}^\bullet$ ) can be generated via direct photolysis of water at 254 nm with a quantum yield of 0.08 for the  $\text{HO}^\bullet$  formation [21]. The oxidation of  $\text{NH}_3$  via a reaction with  $\text{HO}^\bullet$  was reported before, and it led to the formation of  $\text{NO}_2^-$ . It was suggested that the initial reaction proceeds with the hydrogen abstraction with  $\text{HO}^\bullet$  yielding the key intermediate  $\text{NH}_2^\bullet$  (Equation (6)) [22].



Besides light,  $\text{O}_2$  is a necessary reagent, so Equation (7) was proposed to be the overall reaction here [23]. Also, the  $\text{NH}_4^+/\text{NH}_3$  acid–base equilibrium  $\text{pK}_a$  is 9.25, which explains that the oxidation was observed at a more alkaline pH where  $\text{NH}_3$  is the main species.



It is postulated that after the initial oxidation of  $\text{NH}_3$  into  $\text{NO}_3^-/\text{NO}_2^-$ , both compounds reacted to produce  $\text{N}_2/\text{NO}_x$  (see next section), which would explain the total nitrogen decrease. This could be described with a two-step consecutive reaction mechanism where the first reaction ( $\text{NH}_3$  oxidation) is much slower than the second reaction ( $\text{N}_2/\text{NO}_x$  generation), producing a steady-state low concentration of  $\text{NO}_3^-$  and  $\text{NO}_2^-$  during the reaction.

### 3.4. Simultaneous Irradiation of $\text{NO}_2^-$ and $\text{NH}_3/\text{NH}_4^+$

The simultaneous removal of aqueous  $\text{NO}_2^-$  and  $\text{NH}_3$  was achieved via irradiation at pH 10 without the detection of  $\text{NO}_3^-$  (Figure 5). Both compounds (0.75 mM) were removed by 75% in 2.5 h. The kinetic curves obtained for  $\text{NO}_2^-$  and  $\text{NH}_3/\text{NH}_4^+$  were almost identical, indicating that the reaction stoichiometry between  $\text{NO}_2^-$  and  $\text{NH}_3/\text{NH}_4^+$  was 1:1. Moreover, the experimental data adjusted very well to a rate equation with a partial first order for  $\text{NO}_2^-$  and also partial first order for  $\text{NH}_3$  ( $\nu = k [\text{NO}_2^-] [\text{NH}_3]$ ,  $k = 0.5 \text{ M}^{-1} \text{ seg}^{-1}$ ,  $R^2 = 0.9994$ ).

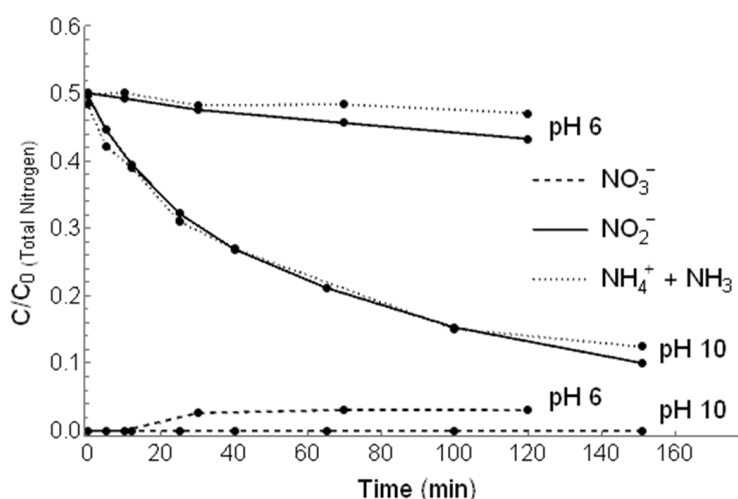


**Figure 5.**  $\text{NO}_3^-$  (dashed lines),  $\text{NO}_2^-$  (solid lines) and  $\text{NH}_3/\text{NH}_4^+$  (dotted lines) profiles vs. time for the irradiation of  $\text{NO}_2^-$  and  $\text{NH}_3/\text{NH}_4^+$  at varying pH conditions. The initial total nitrogen concentration ( $C_0$ ) was 1.5 mM. The solution was purged with argon.

At pH 6, the reaction was significantly slower, and the formation of  $\text{NO}_3^-$  was evidenced as a reaction product without a significant total nitrogen removal. This reaction dependence on pH suggested that  $\text{NH}_3$ , not  $\text{NH}_4^+$ , is the reactant that leads to nitrogen removal.

The mechanism of the photochemical reaction between  $\text{NH}_3$  and  $\text{NO}_2^-$  can be analyzed considering the mechanism of the thermal reaction. One of the key intermediates proposed in the thermal reaction is dinitrogen trioxide ( $\text{N}_2\text{O}_3$ ).  $\text{NH}_3$  reacts with  $\text{N}_2\text{O}_3$  (Equation (8)) through a Substitution Nucleophilic Bimolecular reaction ( $\text{S}_{\text{N}}2$ ) (Figure 6A) [24] where  $\text{NH}_3$  is the nucleophile,  $\text{N}_2\text{O}_3$  the electrophile and  $\text{NO}_2^-$  the leaving group.

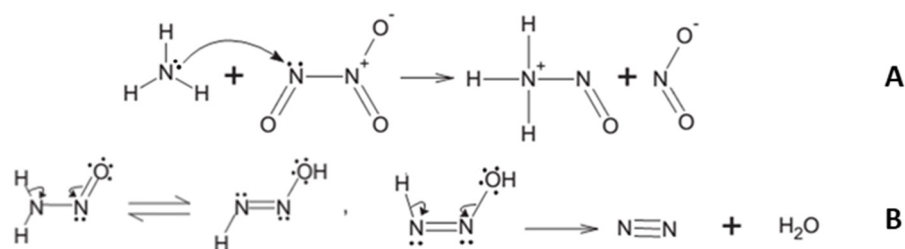


**Figure 6.** Substitution Nucleophilic Bimolecular reaction between  $\text{NH}_3$  and  $\text{N}_2\text{O}_3$  (A) and  $\text{H}_2\text{NNO}$  isomerization and dissociation (B).

The transient compound,  $\text{H}_3\text{NNO}^+$ , quickly converts into nitrosamine ( $\text{H}_2\text{NNO}$ ) (Equation (9)) [24].



And  $\text{H}_2\text{NNO}$  isomerizes into  $\text{HNNOH}$ , which dissociates into the final products  $\text{N}_2$  and  $\text{H}_2\text{O}$  (Equation (10)) [24] (Figure 6B).



As in the thermal reaction,  $\text{N}_2\text{O}_3$  could also be postulated as an intermediate for the photochemical reaction [25]. The final steps of the mechanisms leading to  $\text{N}_2$  would be the same as stated above, but the difference would lie in how  $\text{N}_2\text{O}_3$  is formed. In the

thermal reaction,  $N_2O_3$  is postulated to be generated by the condensation of two molecules of  $HNO_2$  (Equation (11)) [24].

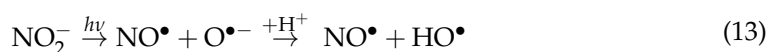


In fact,  $HNO_2$  and  $NH_3$  are the postulated reagents for the thermal reaction where the reaction rate increases at a lower pH [24]. On the contrary, in the photochemical reaction, the postulated reagents are  $NO_2^-$  and  $NH_3$ , and as shown here, the reaction takes place in alkaline media.

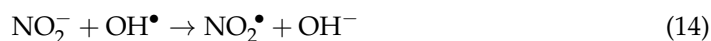
The formation of  $N_2O_3$  via irradiation could be explained by the reaction between  $NO^\bullet$  and  $NO_2^\bullet$  (Equation (12)) [8].



where  $NO^\bullet$  is obtained in the photochemical primary process of  $NO_2^-$  irradiation (Equation (13)) [26]:



and  $NO_2^\bullet$  is generated by the oxidation of  $NO_2^-$  by  $OH^\bullet$  (Equation (14)) [27].



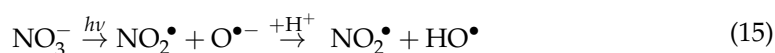
Another important difference is that in the thermal process, the kinetic mechanism is near-second-order in the  $HNO_2$  concentration [24], whereas we showed here that in the irradiation process, the reaction was first-order in the  $NO_2^-$  concentration.

We did not observe a significant reaction in the dark. This could be due to the relatively low total nitrogen concentration (about 1.5 mM) used in these experiments. The thermal reaction is reported to have occurred mainly at concentrations above 100 mM<sup>11</sup>. This agrees with the different reaction mechanisms indicated above.

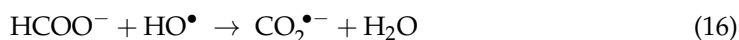
### 3.5. Irradiation of $NO_3^-$ in the Presence of Formic Acid

As shown in previous sections, the irradiation of  $NO_3^-$  and  $NO_2^-$  with a medium-pressure mercury lamp produces reactive nitrogen species (RNS) as intermediates, which in turn yields  $NO_2^-$  as the main product regardless of the initial conditions of pH and oxygenation. To achieve further nitrogen reduction and eventually eliminate it, it is necessary to add another reactant as an electron donor, such as an organic compound.

This is possible because the irradiation of  $NO_3^-$  and  $NO_2^-$ , besides RNS, produces reactive oxygen species (ROS), which are scavenged by organic compounds that are oxidized and mineralized in this way.  $HO^\bullet$  is the main ROS produced as a consequence of the irradiation of  $NO_2^-$  and  $NO_3^-$  (Equations (13) and (15), respectively). Therefore, this irradiation process has also been proposed for the removal of contaminants of emerging concern (CECs) [14].



In particular, it is known that formic acid is oxidized by  $HO^\bullet$ , yielding  $CO_2^{\bullet-}$  as the first intermediate (Equation (16)) [28].



The irradiation of  $NO_3^-$  in the presence of formic acid yielded  $NH_3$  and a loss of total nitrogen at pH 10 (Figure 7). In the beginning of the reaction, a transient peak of  $NO_2^-$  concentration was observed along with a quick fall of the  $NO_3^-$  concentration. Then,  $NH_3$  appeared after a lag period in which a minimum of total nitrogen was observed. This suggested the presence of another nitrogen intermediate that was different from the three main DINs and that was converted into  $NH_3$  more slowly.

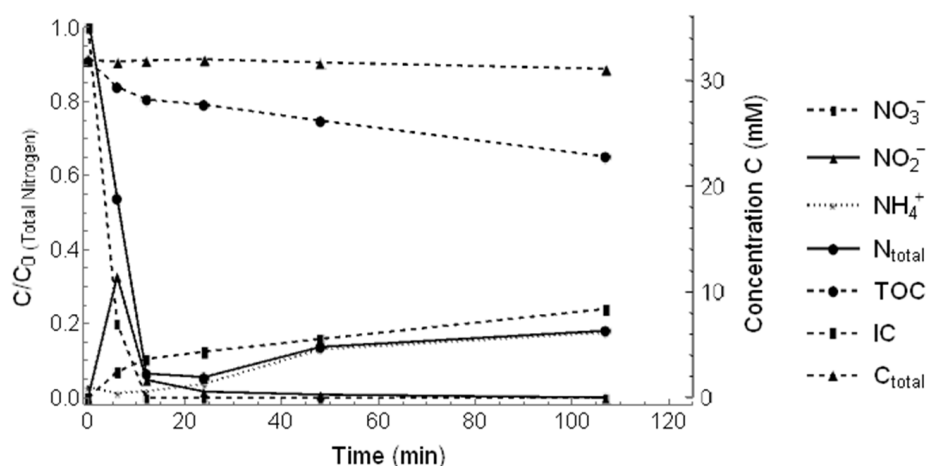


**Figure 7.** Irradiation of  $\text{NO}_3^-$  (1.5 mM) at pH 10 with 30 mM formic acid. The solution was continuously purged with argon.

$\text{NO}_3^-$  removal with formic acid was faster than in the simple irradiation (Section 3.1). Also, the total nitrogen was removed faster than in the simultaneous irradiation of  $\text{NO}_2^-$  and  $\text{NH}_3$  (Section 3.4), evidencing a different mechanism for nitrogen removal. Similar reaction rates were obtained at pH 3 with formic acid. This was another significant difference compared to the irradiation without the electron donor, which had a marked dependence on the pH as shown before.

It is suggested that this new mechanism and the nitrogen intermediates could be initiated by the reaction between  $\text{NO}^\bullet$  and  $\text{CO}_2^{\bullet-}$  (Equation (17)), which are the products of the photolysis of  $\text{NO}_2^-$  (Equation (13)) and the oxidation of formic acid (Equation (16)), respectively [28].



The oxidation of formic acid was also confirmed with the measurement of total organic carbon (TOC). During the reaction, the TOC was reduced steadily along with the formation of inorganic carbon (IC), which showed the mineralization of the formic acid (Figure 7).

Formate has already been tested for the removal of nitrate from groundwater [29], indicating that the environmental application is potentially possible.

#### 4. Conclusions

The irradiation of the principal DIN compounds ( $\text{NO}_3^-$ ,  $\text{NO}_2^-$  and  $\text{NH}_3/\text{NH}_4^+$ ) was performed separately at a relatively low concentration (1.5 mM) with a medium-pressure mercury lamp with main emission bands between 313 and 436 nm. The interconversion of DIN compounds was observed mainly in alkaline media (pH 10–11). In these conditions, it was found that  $\text{NO}_3^-$  is fully converted into  $\text{NO}_2^-$  following first-order reaction kinetics, and  $\text{NH}_3$  was removed from the solution in the presence of oxygen, also yielding a minimum amount of  $\text{NO}_3^-$  and  $\text{NO}_2^-$ . Interestingly, when  $\text{NO}_2^-$  and  $\text{NH}_3$  were irradiated simultaneously, both were removed from the solution in a 1-to-1 mol proportion without the requirement of any other reactant. Finally,  $\text{NO}_3^-$  was reduced to  $\text{NH}_3$  only after the addition of formic acid as an electron donor, also yielding the removal of the DINs from the solution.

The required alkaline media suggested  $\text{NH}_3$  as the active compound instead of  $\text{NH}_4^+$ , and in the case of  $\text{NO}_3^-$  irradiation, it suggested the presence of a reaction intermediate, probably peroxynitrite ( $\text{ONOO}^-$ ), which is unstable in an acidic pH.

It was demonstrated that the DINs could be removed from the solution without introducing a catalyst and by applying a light source emitting in the UV A/B range; therefore, solar irradiation could eventually be applied also. The strategy for DIN removal via irradiation would be to have  $\text{NO}_3^-$  and/or  $\text{NO}_2^-$  mixed with  $\text{NH}_3$  at pH 10–11. If  $\text{NO}_3^-$  and  $\text{NO}_2^-$  are initially absent, they can be obtained via irradiation of  $\text{NH}_3$  in the presence

of oxygen. On the other hand, if  $\text{NH}_3$  is initially absent, it can be obtained via the reduction of  $\text{NO}_3^-$  and/or  $\text{NO}_2^-$  adding an electron donor such as formic acid as shown in this work.

In conclusion, our study demonstrates that direct UV irradiation of DINs presents a promising removal protocol, serving as a valuable complementary approach to enhance existing techniques. Its main advantages lie in its minimal supply requirements, as it solely relies on a UV light source (the protocol can be enhanced by the addition of formate) and eliminates the need for catalysts. On the other hand, it is suggested that formate was oxidized by RNS and ROS produced by the irradiation of nitrate and nitrite. RNS and ROS oxidation have also been proposed as degradation mechanisms of CECs achieving the removal of nitrate and nitrite at the same time.

By offering a simple and sustainable alternative, our findings encourage further exploration and integration of direct UV irradiation in DIN removal strategies, paving the way for more efficient and environmentally friendly pollutant mitigation practices.

**Supplementary Materials:** The following supporting information can be downloaded at: <https://www.mdpi.com/article/10.3390/chemengineering7050079/s1>, Figure S1: Absorption UV–vis spectra of  $\text{NO}_3^-$  and  $\text{NO}_2^-$  measured at pH 10.5 and emission spectrum of the medium-pressure Hg lamp.

**Author Contributions:** Conceptualization, A.M.S. and N.Q.; methodology, A.M.S.; formal analysis, A.M.S. and N.Q.; investigation, A.M.S.; resources, N.Q.; writing—original draft preparation, A.M.S.; writing—review and editing, N.Q.; project administration, N.Q.; funding acquisition, N.Q. All authors have read and agreed to the published version of the manuscript.

**Funding:** This work was supported by Agencia Nacional de Promoción Científica y Tecnológica (ANPCyT, Argentina) PICT project 2018-3114 and Consejo Nacional de Investigaciones Científicas y Técnicas (CONICET) PIP project 11220200101024CO.

**Data Availability Statement:** The data presented in this study are available in the article and the supplementary material.

**Acknowledgments:** The authors thank their corresponding institutions.

**Conflicts of Interest:** The authors declare no conflict of interest. The funders had no role in the design of the study; in the collection, analyses or interpretation of data; in the writing of the manuscript or in the decision to publish the results.

## References

1. Galloway, J.N.; Aber, J.D.; Erisman, J.W.; Seitzinger, S.P.; Howarth, R.W.; Cowling, E.B.; Cosby, B.J. The Nitrogen Cascade. *BioScience* **2003**, *53*, 341–356. [[CrossRef](#)]
2. Nolan, B.T.; Hitt, K.J.; Ruddy, B.C. Probability of Nitrate Contamination of Recently Recharged Groundwaters in the Conterminous United States. *Environ. Sci. Technol.* **2002**, *36*, 2138–2145. [[CrossRef](#)]
3. Galloway, J.N.; Schlesinger, W.H.; Levy, H.; Michaels, A.; Schnoor, J.L. Nitrogen fixation: Anthropogenic enhancement–environmental response. *Glob. Biogeochem. Cycles* **1995**, *9*, 235–252. [[CrossRef](#)]
4. Gruber, N.; Galloway, J.N. An Earth-system perspective of the global nitrogen cycle. *Nature* **2008**, *451*, 293–296. [[CrossRef](#)]
5. Winkler, M.K.; Straka, L. New directions in biological nitrogen removal and recovery from wastewater. *Curr. Opin. Biotechnol.* **2019**, *57*, 50–55. [[CrossRef](#)]
6. van der Star, W.R.L.; Abma, W.R.; Blommers, D.; Mulder, J.-W.; Tokutomi, T.; Strous, M.; Picioreanu, C.; van Loosdrecht, M.C.M. Startup of reactors for anoxic ammonium oxidation: Experiences from the first full-scale anammox reactor in Rotterdam. *Water Res.* **2007**, *41*, 4149–4163. [[CrossRef](#)]
7. Tugaoen, H.O.; Garcia-Segura, S.; Hristovski, K.; Westerhoff, P. Challenges in photocatalytic reduction of nitrate as a water treatment technology. *Sci. Total. Environ.* **2017**, *599–600*, 1524–1551. [[CrossRef](#)]
8. Mack, J.; Bolton, J.R. Photochemistry of nitrite and nitrate in aqueous solution: A review. *J. Photochem. Photobiol. A Chem.* **1999**, *128*, 1–13. [[CrossRef](#)]
9. Vione, D.; Maurino, V.; Minero, C.; Pelizzetti, E. Reactions Induced in Natural Waters by Irradiation of Nitrate and Nitrite Ions. In *The Handbook of Environmental Chemistry; Environmental Photochemistry Part II*; Boule, P., Bahnemann, D.W., Robertson, P.K.J., Eds.; Springer: Berlin/Heidelberg, Germany, 2005; pp. 221–253. [[CrossRef](#)]
10. Wang, Y.; Huang, D.D.; Huang, W.; Liu, B.; Chen, Q.; Huang, R.; Gen, M.; Mabato, B.R.G.; Chan, C.K.; Li, X.; et al. Enhanced Nitrite Production from the Aqueous Photolysis of Nitrate in the Presence of Vanillic Acid and Implications for the Roles of Light-Absorbing Organics. *Environ. Sci. Technol.* **2021**, *55*, 15694–15704. [[CrossRef](#)]

11. Shibuya, S.; Aoki, S.; Sekine, Y.; Mikami, I. Influence of oxygen addition on photocatalytic oxidation of aqueous ammonia over platinum-loaded TiO<sub>2</sub>. *Appl. Catal. B Environ.* **2013**, *138–139*, 294–298. [[CrossRef](#)]
12. Ren, H.-T.; Liang, Y.; Han, X.; Liu, Y.; Wu, S.-H.; Bai, H.; Jia, S.-Y. Photocatalytic oxidation of aqueous ammonia by Ag<sub>2</sub>O/TiO<sub>2</sub> (P25): New insights into selectivity and contributions of different oxidative species. *Appl. Surf. Sci.* **2020**, *504*, 144433. [[CrossRef](#)]
13. Mokhtar, B.; Ahmed, A.Y.; Kandiel, T.A. Revisiting the mechanisms of nitrite ions and ammonia removal from aqueous solutions: Photolysis versus photocatalysis. *Photochem. Photobiol. Sci.* **2022**, *21*, 1833–1843. [[CrossRef](#)]
14. Zhou, S.; Li, L.; Wu, Y.; Zhu, S.; Zhu, N.; Bu, L.; Dionysiou, D.D. UV365 induced elimination of contaminants of emerging concern in the presence of residual nitrite: Roles of reactive nitrogen species. *Water Res.* **2020**, *178*, 115829. [[CrossRef](#)]
15. Wang, J.; Song, M.; Chen, B.; Wang, L.; Zhu, R. Effects of pH and H<sub>2</sub>O<sub>2</sub> on ammonia, nitrite, and nitrate transformations during UV254nm irradiation: Implications to nitrogen removal and analysis. *Chemosphere* **2017**, *184*, 1003–1011. [[CrossRef](#)]
16. APHA; AWWA; WEF (Eds.) Method 4500-NO<sub>3</sub>- E. Cadmium reduction method. In *Standard Methods for the Examination of Water and Wastewater*, 21st ed.; American Public Health Association/American Water Works Association/Water Environment Federation: Washington, DC, USA, 2005.
17. APHA; AWWA; WEF (Eds.) Method 4500-NO<sub>2</sub>- B. Colorimetric method. In *Standard Methods for the Examination of Water and Wastewater*, 21st ed.; American Public Health Association/American Water Works Association/Water Environment Federation: Washington, DC, USA, 2005.
18. APHA; AWWA; WEF (Eds.) Method 4500-NH<sub>3</sub> F. Phenate Method. In *Standard Methods for the Examination of Water and Wastewater*, 21st ed.; American Public Health Association/American Water Works Association/Water Environment Federation: Washington, DC, USA, 2005.
19. Molina, C.; Kissner, R.; Koppenol, W.H. Decomposition kinetics of peroxyxynitrite: Influence of pH and buffer. *Dalton Trans.* **2013**, *42*, 9898–9905. [[CrossRef](#)]
20. Chu, L.; Anastasio, C. Quantum Yields of Hydroxyl Radical and Nitrogen Dioxide from the Photolysis of Nitrate on Ice. *J. Phys. Chem. A* **2003**, *107*, 9594–9602. [[CrossRef](#)]
21. Tomanová, K.; Precek, M.; Múčka, V.; Vyšín, L.; Juha, L.; Čuba, V. At the crossroad of photochemistry and radiation chemistry: Formation of hydroxyl radicals in diluted aqueous solutions exposed to ultraviolet radiation. *Phys. Chem. Chem. Phys.* **2017**, *19*, 29402–29408. [[CrossRef](#)]
22. Huang, L.; Li, L.; Dong, W.; Liu, Y.; Hou, H. Removal of Ammonia by OH Radical in Aqueous Phase. *Environ. Sci. Technol.* **2008**, *42*, 8070–8075. [[CrossRef](#)]
23. Wang, A.; Edwards, J.G.; Davies, J.A. Photooxidation of aqueous ammonia with titania-based heterogeneous catalysts. *Sol. Energy* **1994**, *52*, 459–466. [[CrossRef](#)]
24. Nguyen, D.A.; Iwaniw, M.A.; Fogler, H. Kinetics and mechanism of the reaction between ammonium and nitrite ions: Experimental and theoretical studies. *Chem. Eng. Sci.* **2003**, *58*, 4351–4362. [[CrossRef](#)]
25. Harrison, C.C.; Malati, M.A.; Smetham, N.B. The UV-enhanced decomposition of aqueous ammonium nitrite. *J. Photochem. Photobiol. A Chem.* **1995**, *89*, 215–219. [[CrossRef](#)]
26. Arakaki, T.; Miyake, T.; Hirakawa, T.; Sakugawa, H. pH Dependent Photoformation of Hydroxyl Radical and Absorbance of Aqueous-Phase N(III) (HNO<sub>2</sub> and NO<sub>2</sub><sup>-</sup>). *Environ. Sci. Technol.* **1999**, *33*, 2561–2565. [[CrossRef](#)]
27. Vione, D.; Maurino, V.; Minero, C.; Pelizzetti, E. Phenol photolysis upon UV irradiation of nitrite in aqueous solution I: Effects of oxygen and 2-propanol. *Chemosphere* **2001**, *45*, 893–902. [[CrossRef](#)]
28. Chen, G.; Hanukovich, S.; Chebeir, M.; Christopher, P.; Liu, H. Nitrate Removal via a Formate Radical-Induced Photochemical Process. *Environ. Sci. Technol.* **2019**, *53*, 316–324. [[CrossRef](#)] [[PubMed](#)]
29. Smith, R.L.; Miller, D.N.; Brooks, M.H.; Widdowson, M.A.; Killingstad, M.W. In Situ Stimulation of Groundwater Denitrification with Formate to Remediate Nitrate Contamination. *Environ. Sci. Technol.* **2001**, *35*, 196–203. [[CrossRef](#)] [[PubMed](#)]

**Disclaimer/Publisher's Note:** The statements, opinions and data contained in all publications are solely those of the individual author(s) and contributor(s) and not of MDPI and/or the editor(s). MDPI and/or the editor(s) disclaim responsibility for any injury to people or property resulting from any ideas, methods, instructions or products referred to in the content.